UDC669.017:620.181.4

Development of Mathematical Model for Predicting Transformation of High-Carbon Steel During Cooling on Runout Table and Its Application to On-line Temperature Control of Hot Strip Mill

Masayoshi Suehiro*1 Takashi Oda*2
Takehide Senuma*1 Seiji Konishi*3

Abstract:

A mathematical model for predicting the progress of transformation in high-carbon steel during cooling was developed to improve temperature control accuracy during cooling on the runout table of the hot strip mill. This model was coupled with a temperature computing model that takes the heat of transformation into account, enabling the accurate calculation of strip temperature change on the runout table. The model was also introduced into the strip water cooling control system of the runout table on an actual hot strip mill, markedly improving the water cooling control of high-carbon steel and fully automating strip water cooling on the runout table.

1. Introduction

Sheet steel containing 0.3% or more carbon (high-carbon steel) rises in temperature by the latent heat of transformation when cooled from a high-temperature austenite condition. This rise not only makes it difficult to control the temperature of the high-carbon steel on the hot strip mill, but also causes the steel's metallurgical properties to vary. When the coiling temperature of the strip is controlled on the hot strip mill's runout table, for example, it is normal that the coiling temperature should decrease with increasing flow of cooling water. With high-carbon steel, however, the coiling temperature rises with increasing cooling water flow rate in a manner contrary to the normal situation. Accurate temperature control under these circumstances requires developing a new strip water cooling control system totally different from the conventional coiling temperature control system. To this end, it is necessary to first develop a temperature estimation model that can predict as accurately as possible the temperature history of strip being cooled. Since the temperature rise of the high-carbon steel is caused by the latent heat of transformation, accurate prediction of transformation during cooling is important to enhance the accuracy of temperature computation.

The authors previously developed a model for predicting the transformation of low-carbon steel[1]. Since the principal product of transformation in low-carbon steel during cooling is ferrite, the development of the model focused on transformation from austenite to ferrite. As pearlite is the principal product of transformation in high-carbon steel, it is necessary to develop a model capable of accurately calculating the progress of pearlite transformation in high-carbon steel. From this standpoint, the authors studied transformation from austenite to pearlite in greater detail, developed a model for predicting the progress of transformation, and used the model to predict off-line the phenomena taking place in high-carbon steel on the hot strip mill[2]. The authors also studied the application of the model to on-line control on the hot strip mill and developed a fully automatic strip water cooling control system for use at the runout table of the hot strip mill[3]. This report summarizes the results of work performed to date on the development and application of the model for predicting high-carbon steel transformation of.

*1 Technical Development Bureau *2 Hikari Works
*3 Yawata Works

2. Transformation Prediction Model

2.1 Basic equations

Assuming that a new phase is nucleated at austenite grain boundaries and that the nucleation rate and growth rate of the new phase do not depend on time, Cahn[4] derived the following equation to describe the transformation behavior of the new phase:

$$X=1-\exp\left(-\frac{\pi}{3}ISG^3t^4\right) \quad \cdots\cdots(1)$$

where X is the fraction transformed, I is the nucleation rate, S is the nucleation site area per unit volume, G is the growth rate, and t is the time. Rewriting Eq. (1) in the form of the transformation rate dX/dt and eliminating the time term, we obtain:

$$\frac{dX}{dt}=4\left(\frac{\pi}{3}\right)^{1/4}(IS)^{1/4}(G)^{3/4}\left(\ln\frac{1}{1-X}\right)^{3/4}(1-X) \quad \cdots\cdots(2)$$

Eq. (2) indicates the progress of transformation by nucleation and growth and is applicable when the additivity rule holds for the progress of transformation. When the nucleation sites are entirely covered with new phase (this condition is called site saturation), the transformation proceeds by growth alone. The progress of transformation in this case is expressed as:

$$\frac{dX}{dt}=2SG(1-X) \quad \cdots\cdots(3)$$

These equations can be used to calculate the progress of transformation in a given cooling process. They are theoretically derived, however, and require experimental coefficients when they are actually applied. Table 1 shows the equations derived for calculating the ferrite, pearlite and bainite transformations and the coefficients obtained for the respective transformations[1,2]. The nucleation and growth mechanism and the site saturation mechanism are both used for the ferrite transformation. The nucleation and growth mechanism alone is used for the pearlite transformation. The site saturation mechanism alone is used for the bainite transformation. As shown in **Table 1**, the Zener-Hillert equation[5-7] is used for the growth rate of ferrite and bainite, and the equation based on the control of the pearlite transformation by the volume diffusion of solute carbon in austenite[8] is used for the growth rate of pearlite. The coefficients for ferrite and bainite were determined by using a 0.1 mass% C-1 mass% Mn-0.5 mass% Si steel, and the coefficients for pearlite were determined by using a 0.5 mass% C steel.

2.2 Method for calculating progress of transformation during cooling

The calculation of transformation in the cooling process by Eqs. (1) to (3) is performed as follows. The calculation of transformation from austenite to ferrite starts when the temperature of the strip being cooled reaches the Ae_3 temperature. The Ae_3 temperature is calculated from thermodynamic data[9] under a para-equilibrium condition. The austenite-to-ferrite transformation is governed by the diffusion of solute carbon in austenite. The solute carbon is concentrated in the austenite as transformation progresses. This solute carbon concentration is calculated here as the increase in the average carbon content of the austenite, C_γ, as given by

$$C_\gamma=(C_0-X_F C_\alpha)/(1-X_F) \quad \cdots\cdots(4)$$

where C_0 is the carbon content of the steel, X_F is the volume fraction of austenite transformed to ferrite, and C_α is the solute carbon content of ferrite.

The pearlite transformation is generally assumed to start when the solute carbon content of the austenite reaches the A_{cm} line, which is extrapolated to temperatures below the A_1 temperature on the phase diagram. The actual behavior differs from the assumed behavior. **Fig. 1** shows the transformation temperature

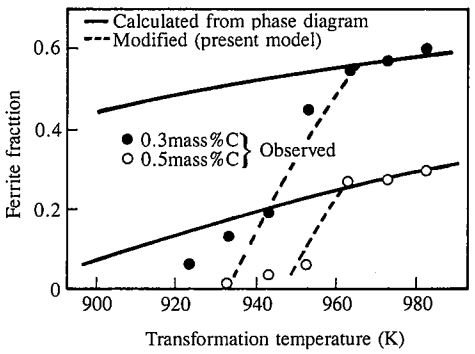

Fig. 1 Relationship between transformation temperature and ferrite fraction (observed and calculated values)

Table 1 Equations and coefficients used in transformation models

Transformation	Basic equation of transformation rate	Factor corresponding to nucleation rate and growth rate	Coefficient
Ferrite	Nucleation and growth $\frac{dX}{dt}=4.046(k_1 SIG^3)^{1/4}\left(\ln\frac{1}{1-X}\right)^{3/4}(1-X)$	$I=T^{-1/2}D\cdot\exp\left(-\frac{k_3}{RT\Delta G_V^2}\right)$ $G^*=\frac{1}{2r}D\frac{C_{\gamma\alpha}-C_\gamma}{C_\gamma-C_\alpha}$	$k_1=17476$ $k_2=8.933\times10^{-12}\exp\left(\frac{21100}{T}\right)$ $k_3=0.957\times10^9$(J³/mol³) $S=6/d_\gamma^4$
	Site saturation $\frac{dX}{dt}=k_2\frac{6}{d_\gamma}G(1-X)$		
Pearlite	Nucleation and growth	$I=T^{-1/2}D\cdot\exp\left(-\frac{k_4}{RT\Delta T^2}\right)$ $G=\Delta T\cdot D\cdot(C_{\gamma\alpha}-C_{\gamma\beta})$	$k_1=2.01\times10^{13}$ $k_4=2.27\times10^9$(J³/mol³) $S=6/d_\gamma$
Bainite	Site saturation	$G^*=\frac{1}{2r}D\frac{C_{\gamma\alpha}-C_\gamma}{C_\gamma-C_\alpha}$	$k_2=6.816\times10^{-4}\exp\left(\frac{3431.5}{T}\right)$

and ferrite volume fraction observed in isothermal transformation experiments. The relationship between the transformation temperature and ferrite volume fraction is indicated by the solid lines in the above assumption and the changes are shown by the circles, which represent the experiments. According to these results, the conditions indicated by the dotted lines were used as the pearlite transformation start conditions. The pearlite transformation start conditions deviate from the Acm line at the low end of the temperature range, possibly because the solute carbon content on the austenite side of the ferrite/austenite phase boundary exceeds the carbon content on the A_{cm} line under local equilibrium.

The bainite transformation start conditions are often discussed in relation to the T_0 temperature[10], but are not yet clear. The experimentally determined bainite transformation start temperature was formulated and adopted by using chemical composition as the variable[1].

3. Combination with Hot Working Model

The transformation behavior of steel is strongly influenced by hot working. This is due to the change in the pre-transformation size of austenite grains to serve as nucleation sites during transformation, introduction of deformation bands, and change in the dislocation density that affects the nucleation and growth rate. The effect of hot working is taken into account by combining the transformation model with the hot working change prediction model developed by Senuma et al[11]. The working-induced strain is converted into the dislocation density and treated as the dislocation density in the hot working model. The present study combines the transformation model with the hot working model by using the austenite grain size calculated by the transformation model and the effective austenite grain size[12] calculated by the hot working model derived from the dislocation density. This combination aims at improving prediction accuracy of transformation progress during cooling in a process involving working before cooling, as is the case with the hot strip mill.

4. Method for Calculating Strip Temperature During Cooling

High-carbon steel produces transformation latent heat during cooling, resulting in rising strip temperature during cooling. This strip temperature change is predicted by a two-dimensional heat transfer equation that takes transformation latent heat into account. The heat transfer equation is

$$\mu C_p \frac{\partial T}{\partial t} = \lambda \frac{\partial^2 T}{\partial x^2} + \lambda \frac{\partial^2 T}{\partial x^2} + \dot{Q} \qquad \cdots\cdots(5)$$

where μ is the density of steel, T is the temperature of steel, λ is the thermal conductivity of steel, and C_p is the specific heat of steel. This specific heat is not usual specific heat, but the specific heat that does not take the magnetic transformation latent heat into account. $\dot{Q}$ is the transformation latent heat and is given by:

$$\dot{Q} = \mu \{ q_l \frac{\partial X}{\partial t} + \frac{\partial}{\partial t}(q_m X) \} \qquad \cdots\cdots(6)$$

where q_l is the lattice transformation latent heat, and q_m is the magnetic transformation latent heat. The value of q_l used here is 16.7 J/g, and the value of q_m is shown in **Fig. 2**. The two-dimensional finite element method (FEM) is used for calculating the strip temperature by Eq. (5).

5. Off-line Application

5.1 Prediction of strip temperature on runout table

Fig. 3 shows the temperature change and transformation behavior of the 0.5 mass% C steel calculated by the model. The temperature change graphs also indicate the strip temperature measured on the runout table of an actual hot strip mill. The observed strip temperature rise during cooling is the same as predicted by the model, and the calculated values agree well with the observed values. The fact that the temperature rise is a phenomenon caused by transformation latent heat can be understood from the comparison of the transformation behavior and temperature change. This finding suggests that the optimum method of cooling the strip on the runout table can be studied off-line by using the model.

5.2 Study of improvement in productivity

To improve hot strip mill productivity, strip speed must be increased. **Fig. 4** shows the cooling curves calculated at the heat transfer coefficient of 1,670 kJ/m²hK during water cooling under the finish rolling temperature of 1,123 K, a coiling temperature of 873 K, and transformation completed 95% or more before coiling. **Fig. 5** shows the cooling curves calculated at the heat transfer coefficient of 5,020 kJ/m²hK. As can be seen from these figures, the strip travel time through the runout table can be shortened from about 12 seconds to about 5 seconds by increasing the heat transfer coefficient from 1,670 to 5,020 kJ/m²hK. In this case, however, the strip may be water cooled to about 800 K below the bainite transformation start temperature (about 823 K for the steel under consideration), resulting in the formation of bainite that lowers steel quality. This risk can be avoided by dividing the water cooling region as shown in **Fig. 6**. In **Fig. 6**, the strip travel time through the runout table does not differ greatly from that shown in **Fig. 5**, but the lowest temperature is above 823 K and this is not the temperature at which bainite transformation starts.

In this way, the model can contribute to higher productivity by establishing the optimum strip cooling pattern.

5.3 Effect of finish rolling temperature

The variation of the finish rolling temperature in the finish rolling train leads to differences in the coiling temperature if the cooling conditions on the runout table are constant. Since the metallurgical properties of high-carbon steel change with the coiling temperature, fluctuations in the finish rolling temperature change the metallurgical properties. In other words, to obtain uniform metallurgical properties, the coiling temperature must be held constant despite fluctuating finish rolling temperatures. **Figs. 7** and **8** show the results of research conducted on this topic. **Fig. 7**

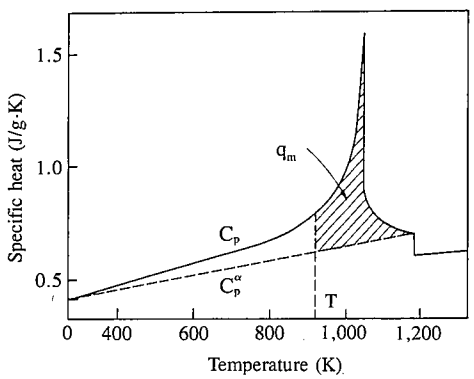

Fig. 2 Specific heat of steel (q_m = magnetic transformation latent heat)

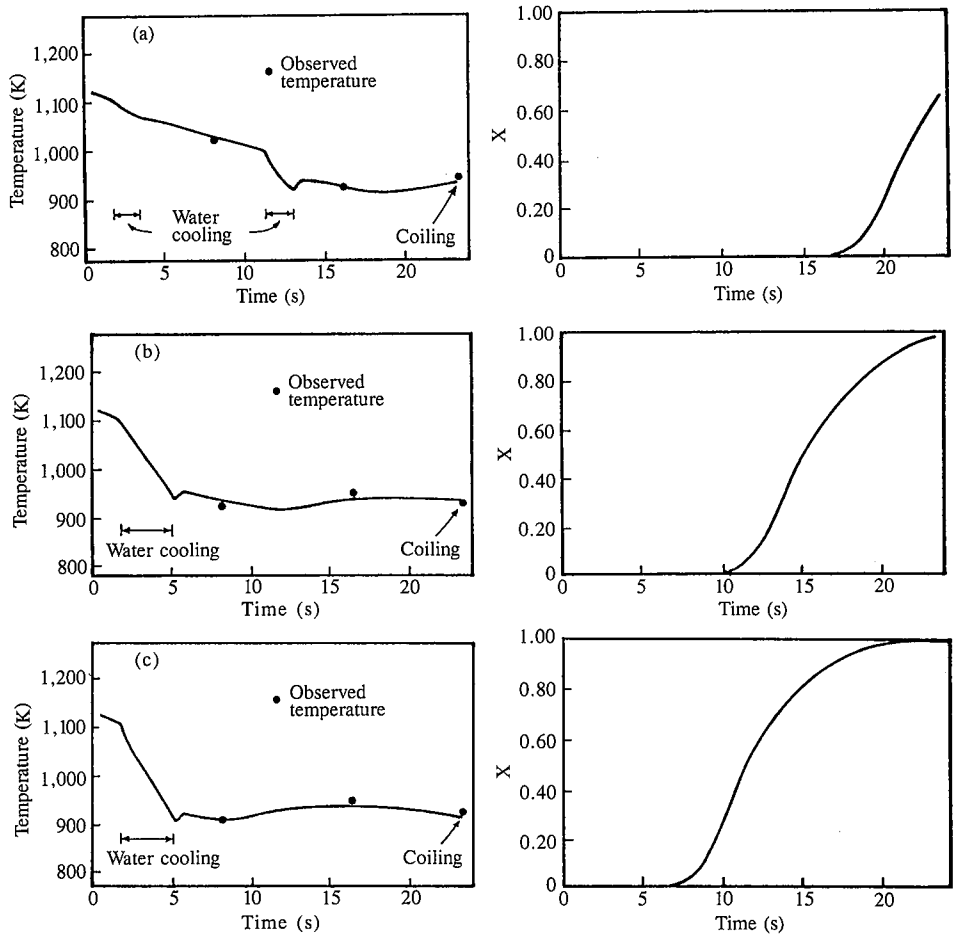

Fig. 3 Strip temperature change and transformation behavior of 0.5 mass% C steel on runout table

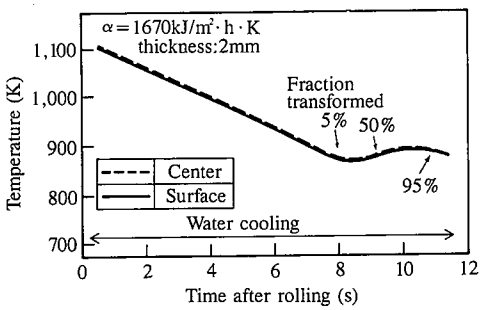

Fig. 4 Strip temperature change of 0.5 mass% C steel on runout table

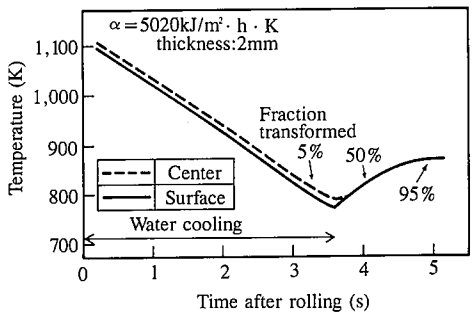

Fig. 5 Strip temperature change of 0.5 mass% C steel on runout table (cooling capacity greater than shown in **Fig. 4**)

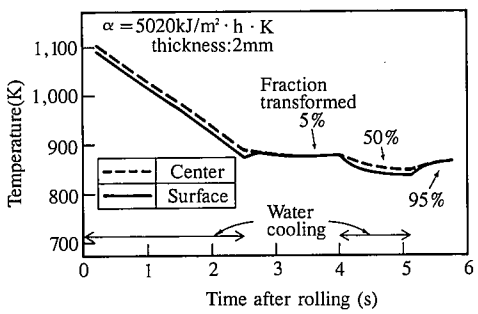

Fig. 6 Strip temperature change of 0.5 mass% C steel on runout table (cooling zones of **Fig. 5** divided further)

shows the cooling curves calculated by changing the finish rolling temperature under constant cooling conditions. **Fig. 8** shows the cooling curves calculated by changing the cooling condition, compensating for finish rolling temperature variations and keeping the coiling temperature constant. As evident from these results, the model can study the cooling conditions required to compensate for finish rolling temperature variations.

6. On-line Application

6.1 Runout table strip water cooling system and water cooling control system

The runout table strip water cooling system at the Yawata Works hot strip mill is schematically illustrated in **Figs. 9** and

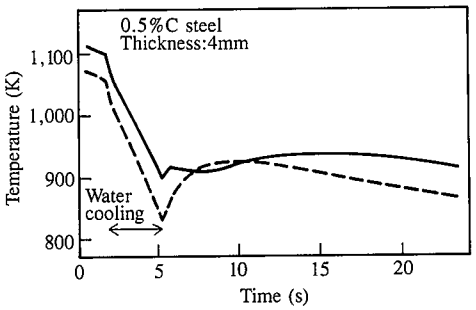

Fig. 7 Runout table strip temperature change with finish rolling temperature

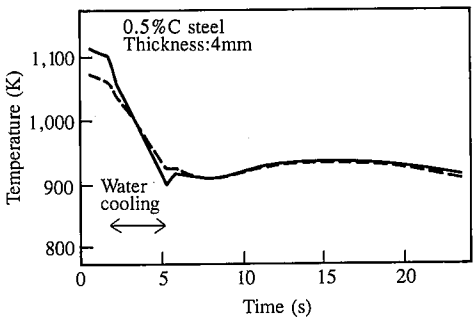

Fig. 8 Runout table strip temperature change with finish rolling temperature (cooling capacity adjusted to ensure constant coiling temperature)

10. A pipe laminar flow method is adopted in both the top and bottom banks, and the entire system is divided into 21 sections, each section equipped with seven headers. To minimize pressure head variations, storage pipes are installed in both the top and bottom parts. To minimize water level variations in the storage pipes, the amount of water to be used in the cooling stage is dynamically predicted, and the speed of the water supply pump is adjusted to keep the variation of the water level within ±20 cm[13]. A control target of 5°C/header is stably achieved by performing the on/off control of the unit valves of specific headers.

Fig. 11 shows the configuration of the strip water cooling control system. To prevent temperature hunting against the change in the rolling speed and to ensure the stability of the control system, the control target (state variable) is set for each of the strip pieces that correspond to the sections of the water cooling system. The observer estimates the actual value of the state variable of the strip piece as it passes each section. The controller calculates the necessary amount of control from the difference between the control target value and the estimated value and calculates the value. The control system can provide rapid convergence to the control target despite the acceleration and deceleration of the strip during cooling, and can easily water cool the strip by minimizing the variation of cooling temperature history. The control target (state variable) should be a physical quantity that can be uniquely determined with respect to a given set of cooling conditions. With carbon steel, for example, the strip temperature is adopted for the state variable as the control target, because the strip temperature in the cooling process is expected to drop evenly. With high-carbon steel, on the other hand, its temperature rises on cooling due to transformation latent heat as already described. That is, the strip temperature does not change

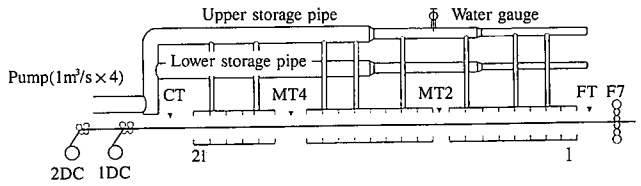

Fig. 9 Overall arrangement of runout table strip water cooling system

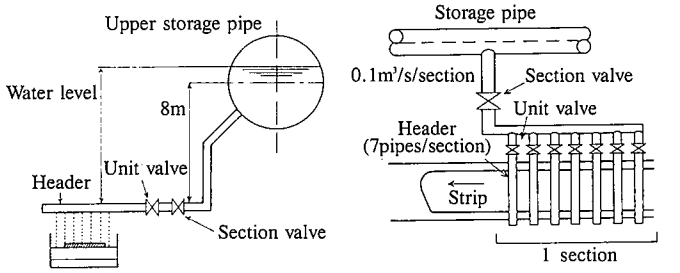

(a) Storage pipe and header (b) Header arrangement in each section

Fig. 10 Details of strip water cooling system

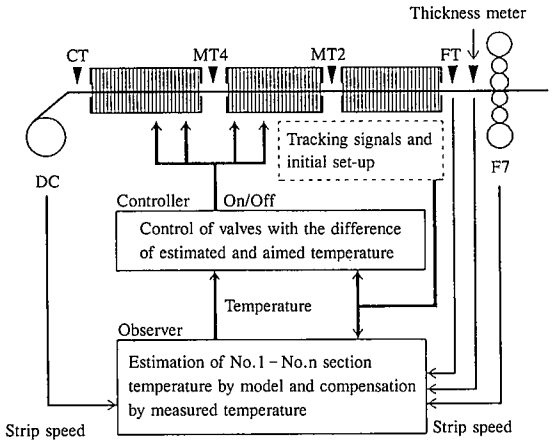

Fig. 11 Strip water cooling control system

evenly. For high-carbon steel, therefore, another quantity that evenly changes must be adopted as the state variable.

The time integration value of cooling heat flux per unit volume, or total amount of heat removed from the strip, E, as expressed by the following equation, is adopted here for high-carbon steel:

$$E = \frac{1}{h}\int_0^t \alpha (T - T_w)\, dt \qquad \cdots\cdots(7)$$

where h is the strip thickness, α is the heat transfer rate, and T_w is the cooling water temperature. Using the amount of heat removed from the strip, E_i, in section i, is represented as:

$$E_i = \frac{1}{h}\alpha_i (T_i - T_w)\, t_i \qquad \cdots\cdots(8)$$

$$E = \Sigma E_i \qquad \cdots\cdots(9)$$

Fig. 12 shows the change in the strip temperature on the runout table, progress of transformation, and change in the total heat removed from the strip. It is evident that the total heat removed changes even when the strip temperature is increased by

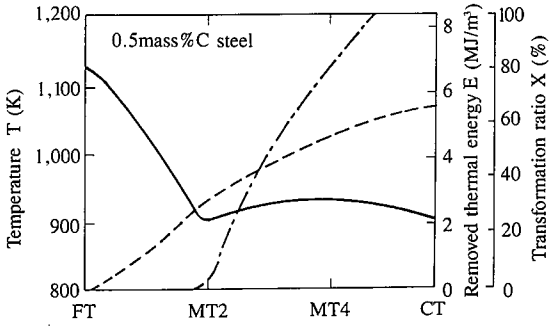

Fig. 12 Strip temperature history and total heat removed during cooling

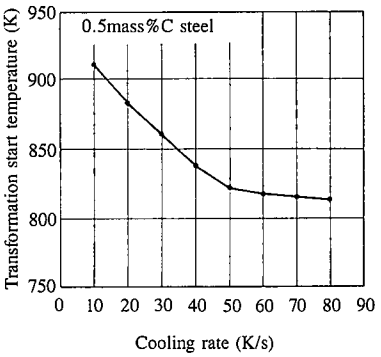

Fig. 13 Relationship between cooling rate and transformation start temperature

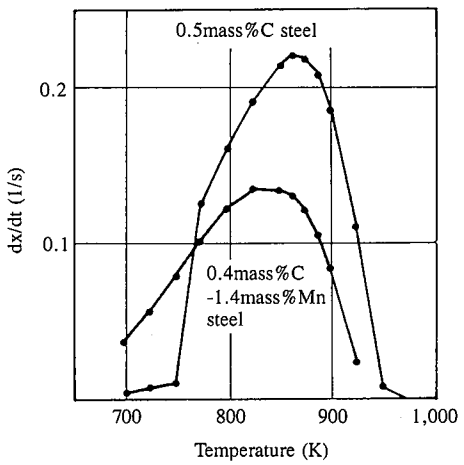

Fig. 14 Relationship between transformation temperature and average transformation rate

transformation latent heat. By taking the total heat removed during coiling as the control target, whether or not transformation is completed can be easily selected as the water cooling criterion during setup. The values shown in **Fig. 12** were calculated not by the method already described, but by the on-line transformation progress calculation model and temperature estimation model described next.

6.2 On-line transformation model and temperature estimation model

Since real-time calculation is necessary on-line, a model simplified to such a degree that its accuracy is not lowered for actual operation was used in place of the transformation model described previously.

The simplified model consists of: (1) a model for calculating the start of transformation; (2) a model for calculating the progress of transformation; and (3) a model for calculating the finish of transformation. The start of transformation was determined from the relationship between the cooling rate and transformation start temperature as shown in **Fig. 13**. Continuous cooling transformation (CCT) curves were prepared for some representative steels, and their transformation start temperature was obtained according to the cooling rate. For other steels, CCT curves were not measured, but the temperature at which the transformation fraction reached 5% was calculated as the transformation start temperature by the above-mentioned transformation prediction model. The addition of hot rolling conditions is necessary for the calculations to be performed by the previously mentioned transformation prediction model. The target values of specific steels were used as the hot rolling conditions. The transformation rate is required by the model for calculating the progress of transformation. The transformation rate from the start of transformation (5%) to the finish of transformation (95%) was obtained as the average transformation rate at each temperature. This value was also obtained by measuring time-temperature-transformation (TTT) curves for the representative steels and was calculated by the above-mentioned transformation prediction model for the other steels. **Fig. 14** shows the relationship between the transformation rate and temperature of the 0.5 mass% C steel and 0.4 mass% C-1.4 mass% Mn steel. The transformation was assumed to be finished when the total transformation fraction reached 1.0.

The strip temperature during cooling was calculated not by the above-mentioned two-dimensional heat transfer equation, but by Eqs. (10) and (11), as these equations are more suited for on-line computation.

$$C_p\mu h\frac{dT}{dt}-h\dot{Q}=-\alpha(T-T_w) \qquad \cdots\cdots(10)$$

$$T_i=T_{i-1}+\frac{h}{\alpha}\dot{Q}\{1-\exp(\frac{\alpha t}{C_p\mu h})\}$$

$$-(T_{i-1}-T_w)\{1-\exp(\frac{\alpha t}{C_p\mu h})\} \qquad \cdots\cdots(11)$$

6.3 On-line control system

To achieve automation, high-carbon steel strip water cooling control system was added to the previously mentioned on-line water cooling control system to achieve automation. **Fig. 15** shows the functional configuration of the system. The system comprises: the function of determining the target value of the total heat removed from the strip in each cooling section during initial setup; the function of converting the difference between the target value and actual value into a corresponding cooling water flow rate; the function of correcting in real time the target value of the total heat removed in response to the change in the rolling finish temperature (FT) during rolling; and the function of correcting the heat transfer coefficient in the model by feedback on the basis of the difference between the target value and actual value of the coiling temperature (CT). The progress of transformation in high-carbon steel is difficult to judge from the interme-

diate strip temperatures (MT2 and MT4). The readings of the intermediate strip pyrometers are used to judge the appropriateness of such physical properties for the control purpose as the transformation start temperature and transformation rate, but not for on-line control. The new control system has succeeded in controlling the coiling temperature with high accuracy despite the variations in rolling speed, finish rolling temperature, and other rolling conditions.

6.4 Results of on-line application

Fig. 16 shows the results of on-line strip temperature calculations made by the model. The strip temperatures measured with the intermediate strip pyrometers (MT2 and MT4) and coiling pyrometer are also shown in **Fig. 16**. The calculated values agree well with the measured values.

Fig. 17 compares the estimated and measured values of the

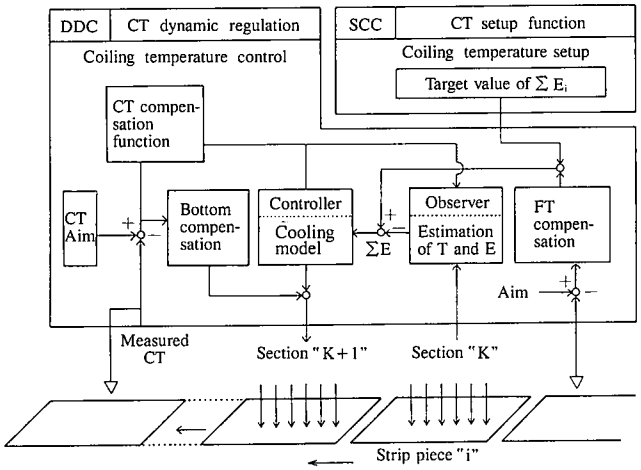

Fig. 15 On-line strip water cooling control system for high-carbon steel

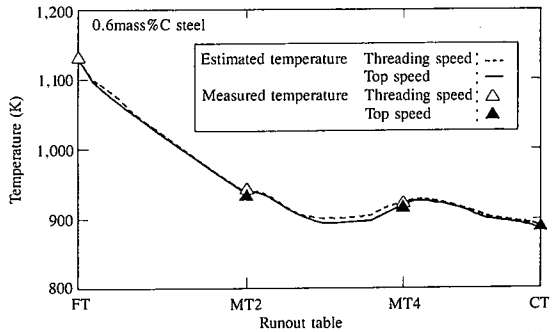

(a) Temperature control results before and after zoom rolling

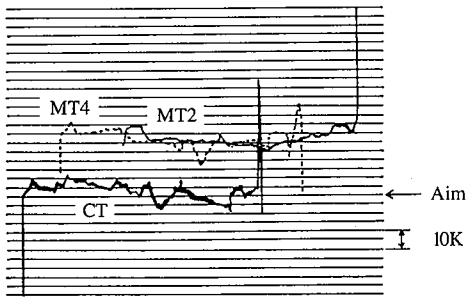

(b) Temperature control results along entire length of coil

Fig. 16 Temperature control results

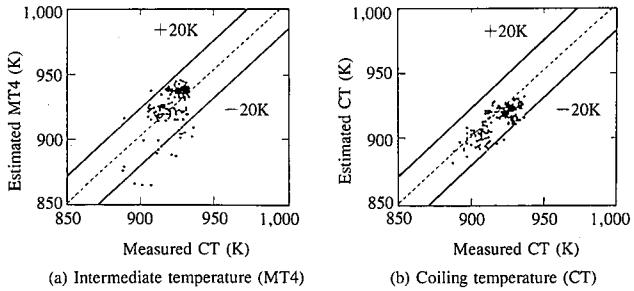

(a) Intermediate temperature (MT4) (b) Coiling temperature (CT)

Fig. 17 Temperature estimation accuracy

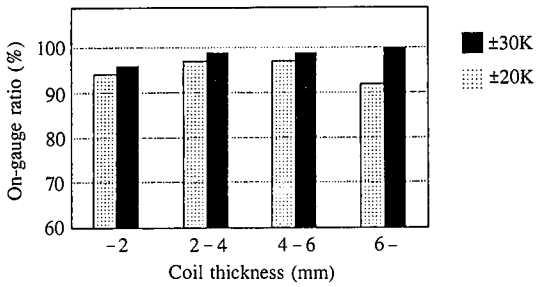

Fig. 18 Temperature hit ratio

intermediate temperature (MT4) and coiling temperature (CT) on the runout table. It was confirmed that temperature estimation accuracy can be held within ±20°C by taking transformation latent heat into account. The temperature hit ratio along the entire length of strip was 96% or more with respect to ±30°C as shown in **Fig. 18**.

7. Conclusions

A mathematical model was developed for calculating the progress of transformation in high-carbon steel during cooling and was applied to predict the progress of transformation and the change in the strip temperature on the runout table of an actual hot strip mill. The temperature rise from transformation latent heat in high-carbon steel during cooling was successfully simulated by the model. The calculated values of strip temperature agreed well with the measured values. It is thus considered feasible to optimize the cooling conditions of strip on the runout table by performing off-line computer simulation with the model.

The model was simplified and introduced into the on-line strip water cooling control system of the hot strip mill runout table. Control with good follow-up in response to the changes in the rolling speed and finish rolling temperature was achieved by changing the state variable as the control target from the strip temperature to the total amount of heat removed from the strip. As a result, the controlled water cooling of high-carbon steel was markedly improved, and fully automatic strip water cooling was accomplished.

References

1) Suehiro, M., Senuma, T., Yada, H., Matsumura, Y., Ariyoshi, T.: Tetsu-to-Hagané. 73, 1026 (1987)
2) Suehiro, M., Senuma, T., Yada, H., Sato, K.: ISIJ Int. 32, 433 (1992)
3) Oda, T., Kondo, Y., Konishi, S., Murakami, O., Suehiro, M., Yabuta, T.: Tetsu-to-Hagané. 81, 191 (1995)
4) Cahn, J.W.: Acta Metall. 4, 449 (1956)
5) Zener, C.: Trans. AIME. 167, 550 (1946)
6) Hillert, M.: Jernkontrets Ann. 141, 757 (1957)

7) Kaufman, L., Radcliffe, S.V., Cohen, M.: Decomposition of Austenite by Diffusional Processes. Zackay, V.F., Aaronson, H.I., Eds. Interscience Publishers, New York, 1962, p. 313
8) Hillert, M.: Decomposition of Austenite by Diffusional Processes. Zackay, V.F., Aaronson, H.I., Eds. Interscience Publishers, New York, 1962, p. 197
9) Uhrenius, B.: Hardenability Concepts with Applications to Steel. Doane, D.V., Kirkaldy, J.S., Eds. TMS-AIME, 1978, p. 28
10) Bhadeshia, H.K.D.H.: Acta Metall. 29, 1117 (1981)
11) Senuma, T., Yada, H., Matsumura, Y., Nimura, T.: Tetsu-to-Hagané. 70, 2112 (1984)
12) Suehiro, M., Sato, K., Tsukano, Y., Yada, H., Senuma, T., Matsumura, Y.: Trans. Iron Steel Inst. Jpn. 27, 439 (1987)
13) Kondo, Y., Konishi, S., Manabe, K., Kawahara, O.: CAMP-ISIJ. 2, 359 (1992)